Characterization and source regions of 51 high-CO events observed during Civil Aircraft for the Regular Investigation of the Atmosphere Based on an Instrument Container (CARIBIC) flights between south China and the Philippines, 2005–2008

S. C. Lai,[1,2] A. K. Baker,[1] T. J. Schuck,[1] F. Slemr,[1] C. A. M. Brenninkmeijer,[1] P. van Velthoven,[3] D. E. Oram,[4] A. Zahn,[5] and H. Ziereis[6]

Received 8 June 2011; revised 2 August 2011; accepted 4 August 2011; published 22 October 2011.

[1] Carbon monoxide (CO) and other atmospheric trace constituents were measured from onboard an Airbus 340-600 passenger aircraft in the upper troposphere (UT) between south China and the Philippines during Civil Aircraft for the Regular Investigation of the Atmosphere Based on an Instrument Container (CARIBIC) flights from May 2005 until March 2008. A total of 132 events having CO enhancements were observed in the UT over the region during the 81 CARIBIC flights from Frankfurt, Germany, to Manila, Philippines, with a stopover in Guangzhou, China. Among these, 51 high-CO events with enhancements more than 50 ppb above background were observed. For these events enhancements ranged from 52.7 to 221.3 ppb and persisted for 3 to 78 min (~40 to 1200 km), indicating an influence of strong pollution from biomass/biofuel/fossil fuel burning on the trace gas composition of the UT. Back trajectory analysis shows that south China, the Indochinese Peninsula, and the Philippines/Indonesia are the main source regions of the high-CO events. The composition of air parcels originating from south China was found to be primarily influenced by anthropogenic urban/industrial emissions, while emissions from biomass/biofuel burning contributed substantially to CO enhancements from the Indochinese Peninsula. During the Philippines/Indonesia events, air parcel composition suggests contributions from both biomass/biofuel burning and urban/industrial sources. Long-range transport of air parcels from northeast Asia and India also contributed to CO enhancements in the UT over the region. The general features of regional influence, typical cases, and the contributions of biomass/biofuel burning and anthropogenic emissions are presented and discussed to characterize the air parcels during the observed high-CO events.

Citation: Lai, S. C., A. K. Baker, T. J. Schuck, F. Slemr, C. A. M. Brenninkmeijer, P. van Velthoven, D. E. Oram, A. Zahn, and H. Ziereis (2011), Characterization and source regions of 51 high-CO events observed during Civil Aircraft for the Regular Investigation of the Atmosphere Based on an Instrument Container (CARIBIC) flights between south China and the Philippines, 2005–2008, *J. Geophys. Res.*, *116*, D20308, doi:10.1029/2011JD016375.

1. Introduction

[2] Carbon monoxide (CO) is emitted primarily from incomplete combustion during the burning of biomass/biofuel and fossil fuel, and is also the product of the oxidation of atmospheric hydrocarbons [*Bergamaschi et al.*, 2000; *Brenninkmeijer et al.*, 1999; *Logan et al.*, 1981]. It is a chemically important trace gas in the atmosphere, and influences the oxidation capacity of the troposphere through reaction with the hydroxyl radical (OH) [*Novelli*, 1999; *Novelli et al.*, 1992]. Because of its boundary layer sources and its lifetime of up to several months, CO can be used as a tracer for lower-tropospheric pollution and its transport to higher levels. Regular ground based measurements of CO are conducted at many locations around the world, importantly the NOAA and World Meteorological Organization (WMO) Global Atmosphere Watch networks. Results of CO monitoring are increasingly available, allowing for the construction of a more complete picture of CO on the global scale. Besides in situ measurements at the surface, great

[1]Max Planck Institute for Chemistry, Air Chemistry Division, Mainz, Germany.
[2]Now at South China University of Technology, School of Environmental Science and Engineering, Guangzhou University City, Guangzhou, China.
[3]Royal Netherlands Meteorological Institute, De Bilt, Netherlands.
[4]National Centre for Atmospheric Science, School of Environmental Sciences, University of East Anglia, Norwich, UK.
[5]Institut für Meteorologie und Klimaforschung, Karlsruhe, Germany.
[6]Institut für Physik der Atmosphäre, Deutsches Zentrum für Luft- und Raumfahrt, Wessling, Germany.

0148-0227/11/2011JD016375

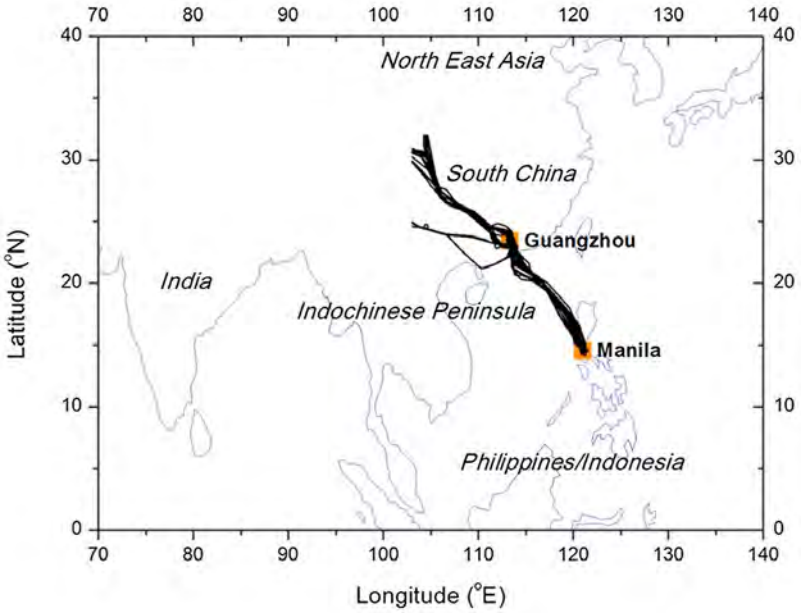

Figure 1. Civil Aircraft for the Regular Investigation of the Atmosphere Based on an Instrument Container (CARIBIC) flight tracks over the region between south China (defined as east of 103°E and south of 32°N) and the Philippines.

progress has been made to better characterize its variable distribution using satellite and aircraft observations [*Brioude et al.*, 2008; *Deeter et al.*, 2003; *Heald et al.*, 2003; *Matsueda and Inoue*, 1999; *Mühle et al.*, 2002; *Park et al.*, 2009]. However, systematic, long-term, in situ measurements of CO in the upper troposphere (UT) are relatively rare. Only the use of passenger aircraft, namely the Civil Aircraft for the Regular Investigation of the Atmosphere Based on an Instrument Container (CARIBIC), Comprehensive Observation Network for Trace Gases by Airliner (CONTRAIL) and Measurement of Ozone and Water Vapor by Airbus in Service Aircraft (MOZAIC) projects, has led to a broader database in this respect [*Brenninkmeijer et al.*, 2007; *Matsueda and Inoue*, 1999; *Nedelec et al.*, 2005]. The large suite of trace gases and aerosol parameters measured by CARIBIC provides the means by which to identify the emission regions and sources of atmospheric CO.

[3] Mixing ratios of CO reported here were measured as part of the CARIBIC (www.caribic-atmospheric.com) research project, which is designed to conduct regular, long-term, long-range, detailed observations in the free troposphere and upper troposphere/lower stratosphere (UT/LS) using a passenger aircraft. Observations are made using a fully automated instrumented container (1.6 tons) installed onboard a Lufthansa Airlines Airbus 340–600. Real time trace gas and aerosol measurements, collection of aerosol and whole air samples, and remote sensing measurements using DOAS are conducted on a near monthly basis [*Brenninkmeijer et al.*, 2007]. For the period between May 2005 and March 2008, data are available from 40 intercontinental flights between Frankfurt and Guangzhou (FRA ↔ CAN) and 41 regional flights between Guangzhou and Manila (CAN ↔ MNL). As one of the most densely populated and fastest growing regions of the world, Southeast Asia has garnered considerable attention as a source of anthropogenic pollutants. Many research campaigns have examined certain aspects of pollution outflow from this region, but these campaigns are usually short in duration and highly specialized in focus, and as such are unable to provide long-term information about pollution reaching the UT. Here we focus on pollution events and air parcels with enhanced CO mixing ratios observed in the UT over the region between south China and the Philippines (Figure 1). In the present work we present an analysis of the entire period, spanning over 2 years. The objective is to characterize polluted air parcels using additional trace gases and attribute them to the different source regions and types of emissions.

2. Methods

2.1. Flights and Region

[4] Measurements under consideration here were made during the CARIBIC flights FRA ↔ CAN and CAN ↔ MNL between May 2005 and March 2008. Altogether, data from 81 flights have been examined. In this paper we discuss only data obtained during the easternmost sections of FRA ↔ CAN flights (defined by latitude <32°N and longitude >103°E) and over the South China Sea during CAN ↔ MNL flights, as shown in Figure 1. In order to study only the upper troposphere, data measured below 7 km (indicating aircraft descent or ascent from an airport) were not considered in the analysis. We also excluded air parcels with potential vorticity (PV) greater than 1.5 PVU (10^{-6} K kg^{-1} m^2 s^{-1}), which suggest lower-stratospheric influence.

2.2. Measurements

[5] Carbon monoxide was measured with a temporal resolution of 1 s using a modified commercial CO analyzer (Model AL 5002, Aero-Laser, Garmisch-Partenkirchen, Germany)

based on vacuum ultraviolet fluorescence [*Brenninkmeijer et al.*, 2007]. The CO scale used prior to July 2010 [*Lai et al.*, 2010; *Slemr et al.*, 2009] was systematically biased to lower values over the range of 0 to 250 ppbv, as was confirmed by a recent round robin laboratory intercomparison organized by NOAA-ESRL and Global Atmosphere Watch (GAW) (WMO). The CO data reported here are now based on the NOAA-ESRL 2004 scale and are 5.4% higher than the values we published previously. The scale correction has negligible influence on the classification and the number of identified pollution events. For the reporting of CO mixing ratios we refer to the new GAW guidelines on CO measurements [*Global Atmosphere Watch*, 2010].

[6] Other measurements in CARIBIC include continuous ozone (O_3; UV absorption, resolution 4 s), total reactive nitrogen (NO_y; chemiluminescence, resolution 1 s), submicrometer aerosols (Condensation Particle Counters, >4 nm (N_4) and >12 nm (N_{12}) diameter, resolution 2 s), total gaseous mercury (TGM) (enrichment and atomic fluorescence, resolution 10 min), acetonitrile (CH_3CN) and acetone (CH_3COCH_3) (Proton Transfer Reaction Mass Spectrometry (PTRMS), resolution 1 min) [*Brenninkmeijer et al.*, 2007]. Whole air samples were collected in glass cylinders over time periods of about one minute. Sampling intervals were equidistant to distribute the samples uniformly over the length of the flight. Typically one sample was collected over south China and three samples were collected between Guangzhou and Manila. A total of 171 whole air samples were collected in the region of interest during all 81 flights.

[7] The air samples were analyzed in the laboratory for greenhouse gases, nonmethane hydrocarbons and halocarbons. Greenhouse gases were measured at the MPIC using gas chromatography coupled with flame ionization detection (GC-FID; CO_2 and CH_4) and electron capture detection (GC-ECD; N_2O, SF_6) [*Schuck et al.*, 2009]. Nonmethane hydrocarbons (NMHCs) were also analyzed at the MPIC, using GC-FID [*Baker et al.*, 2010]. Halocarbons were analyzed by gas chromatography – mass spectrometry (GC-MS) at the University of East Anglia, United Kingdom [*O'Sullivan*, 2007; *Oram et al.*, 2011].

[8] Flight parameters including latitude, longitude, pressure, altitude and temperature were provided by the aircraft ARINC 428 system. The PV values and back trajectories were calculated using data from the European Center for Medium-Range Weather Forecasts (ECMWF) and the model of the Royal Netherlands Meteorological Institute (KNMI) (http://www.knmi.nl/~velthove/). Meteorological analyses and back trajectory calculations are performed for each flight and are based on ECMWF reanalyzed data determined along the flight track [*Scheele et al.*, 1996; P. van Velthoven, 2011, Meteorological analysis of CARIBIC by KNMI, http://www.knmi.nl/samenw/campaign_support/CARIBIC/]. Wind fields are calculated at a 1° × 1° resolution for 6 h, and meteorological data along the flight track are interpolated from wind field data at 1 min time steps. The KNMI TRAJKS model is used to calculate 5 d back trajectories along the flight track at 3 min intervals [*Scheele et al.*, 1996]. Additional 8 d back trajectories are calculated for the individual whole air samples. All back trajectories along the flight route were checked for cloud contact during the preceding 2 d using a FORTRAN algorithm [*Weigelt et al.*, 2009] overlaying back trajectories and satellite cloud images from the International Satellite Cloud Climatology Project (ISCCP, http://isccp.giss.nasa.gov/). Cloud contact analysis combining back trajectory analysis and satellite cloud image was conducted to investigate the influence of convection through the contact of air parcels and clouds. It has been suggested to be a powerful tool to analyze the air parcel originating from local sources. Here we looked through the previous 2 d cloud contact data for each event to search for indications of recent local convection.

[9] Fire maps were obtained from the Fire Information for Resource Management System (FIRMS) web fire mapper based on the Moderate Resolution Imaging Spectroradiometer (MODIS) observation on NASA's Terra satellite (http://firefly.geog.umd.edu/firemap/). Satellite cloud images were from the Space Science and Engineering Center, University of Wisconsin-Madison (SSEC).

3. Results and Discussion

3.1. CO Events

[10] During CARIBIC flights between south China and Manila, highly variable mixing ratios of tropospheric CO were observed, ranging from 59.3 to 322.4 ppb, indicating frequent encounters with polluted air parcels. Because of the complexity of temporal CO patterns during the flights, interpretation of CO events first requires a definition of the background CO mixing ratio. For this, we take the median CO value as it is less influenced by extremely high and low mixing ratios [*Rudolph*, 1995]. Background CO levels over the South China Sea were determined from CO values measured during the flight sections between Guangzhou and Manila. The altitudes of incoming flights to Guangzhou (10–12 km) were systematically higher than that of the outgoing flights (8–10 km). To account for this difference, background CO levels over south China were based on the CO data collected during individual flights. Having defined background values this way, we define "CO events" as those periods having durations greater than 1 min during which maximum CO mixing ratios exceeded the background CO value by more than 10 ppb (ΔCO >10 ppb). Altogether 132 CO events were observed during the 81 CARIBIC flights; of these, 62% of events had CO enhancements between 10 and 50 ppb, 32% had enhancements of 50 to 150 ppb and the remaining 6% had enhancements of over 150 ppb (Figure 2).

3.2. High-CO Events

[11] For further analysis we focus on high-CO events with ΔCO of >50 ppb. These substantial enhancements were chosen to increase the possibility of examining events for which clear source signatures can be established. A total of 51 such high-CO events were observed during the 81 selected CARIBIC flights. Peak mixing ratios of CO ranged from ~137.0 to ~321.5 ppb, with enhancements ranging from 52.7 to 221.3 ppb. The duration of high-CO events ranged from 3 to 78 min (Figure 2b) corresponding to flight distances from ~40 km to ~1200 km. Such strong pollution in the UT has also been observed during previous aircraft studies [*Brioude et al.*, 2008; *Nedelec et al.*, 2005] and the observation of high CO over long distances suggests the existence of polluted quasi-horizontal layers [*Newell et al.*, 1999]. 70% of the high-CO events were observed at cruis-

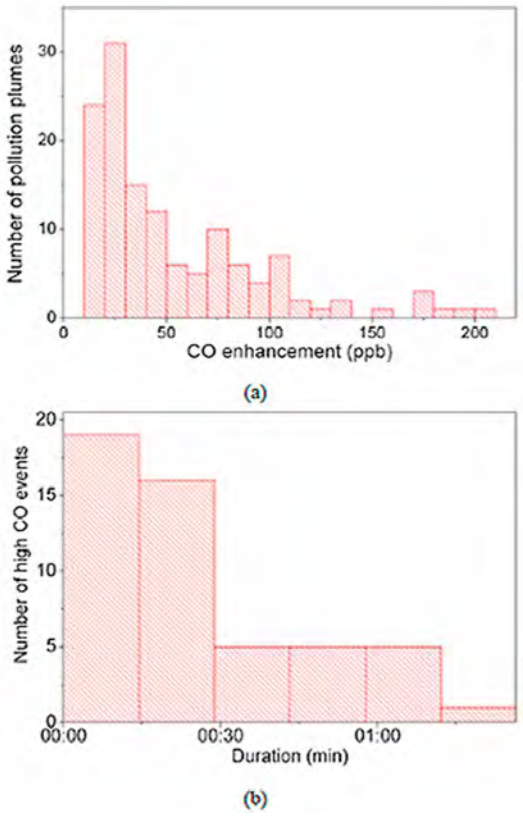

Figure 2. Histogram of (a) CO enhancements during observed CO events (CO >10 ppb) and (b) duration of high-CO events (CO >50 ppb). Event durations were between 3 and 78 min.

ing altitudes of 9–11.5 km, but high-CO events were also encountered at 7–9 km during ascending and descending phases. However, most of the high-CO events observed during ascent and descent were of short duration, probably because quasi-horizontal pollution layers were intersected by the aircraft.

[12] Of the 51 high-CO events, 26 were observed during flights over south China, while 25 were observed over the South China Sea. The number of high-CO events was different for the incoming and outgoing flights to/from Guangzhou: 16 high-CO events were observed during the incoming flights to Guangzhou at an average cruising altitude of ~11.5 km, of which 10 were encountered above 10 km, and 10 high-CO events were encountered during outgoing flights at altitudes of 7.4–9.6 km. The difference of high-CO event frequencies might be related to the different local times; incoming flights took place between 16:00 and 18:00 local time, thus after and or during periods when convection is typical, whereas the outgoing flights from Guangzhou usually took off around midnight when local convection is usually weak or absent.

[13] CO enhancements observed over south China flights varied between 52.7 and 221.3 ppb. Extreme enhancements with ΔCO >150 ppb were observed during 5 flights and 4 of these were observed at a cruising altitude of ~11.5 km, indicating that strong pollution reaches high altitudes in the UT over south China. The CO enhancements between Guangzhou and Manila (CAN ↔ MNL) ranged from ~50 to ~190 ppb. However, these enhancements were generally not as large as those encountered over south China; only 7 of the 25 events had CO enhancements >100 ppb. The altitudes of the events were between 7 and 12 km, with most encountered at altitudes of >9.5 km. No significant difference in cruising altitude between incoming and outgoing flights to/from Guangzhou was found.

[14] The seasonal dependence of the frequency of high-CO events was also investigated. Over south China, no seasonal dependence was found, although there were fewer events in June and September, likely the result of fewer flights during these months than in other months. However, a seasonal dependence of high-CO events can be found in the UT between Guangzhou and Manila with April and October having the most frequent high-CO events.

[15] The air parcels corresponding to high-CO events can be further characterized using results from simultaneous measurements of various trace gases (O_3, NO_y, acetone, acetonitrile, TGM, water vapor) and aerosols (N_{4-12} and N_{12}), and by the analyses of whole air samples. As whole air samples were collected at fixed intervals, samples were not always collected during high-CO events. Altogether, a total of 34 air samples were collected during 26 high-CO events, or between 1 and 3 samples per event. Different tracers are used for characterization, such as CH_3Cl and acetonitrile for biomass/biofuel burning, O_3 for plume evolution, C_2Cl_4 for industrial/urban anthropogenic emissions, and their correlations with CO, as well as relationships between different tracers, are used to identify possible sources responsible for the events.

3.3. Regional Influence

[16] To understand regional input to high-CO events, 5 d back trajectory analysis is used to classify the source region of each event. When most or all of the back trajectories for a specific event originate from a certain region, we classify it as an event from this region. Trajectories for the whole set of 51 high-CO events indicate three major source regions and the events are classified accordingly as south China events (SCE), Indochinese Peninsula events (ICE), and Philippines/Indonesia events (PIE), and 46 of the 51 high-CO events can thus be unambiguously classified. The remaining 5 events have been influenced by transport from a broad region of North China, Korea and Japan, and India. The events originating from these two regions are classified as northeast Asia Events (NEAE) and India Events (INE), respectively.

[17] During flights over south China, the origin of the intersected high-CO events can be classified as either SCE or ICE. On the other hand, during flights over the South China Sea high-CO events were traceable to all 5 source regions. Enhancements of traces gases during the high-CO events from the three main source regions (south China, Indochinese Peninsula and Philippines/Indonesia) are shown in Table 1.

3.3.1. Source Signatures From Different Regions

[18] High-CO events were further investigated to understand chemical signatures of air parcels related to source types and source regions, taking anthropogenic emissions (mainly referring to urban and industrial emissions, such as fossil fuel and solvent use) and biomass/biofuel burning into account. Clearly distinguishing between elevated CO from

Table 1. Enhancements of Atmospheric Trace Gases During High-CO Events From the Three Main Source Regions and Three Source Types Identified During Civil Aircraft for the Regular Investigation of the Atmosphere Based on an Instrument Container (CARIBIC) Flights Between South China and the Philippines[a]

Compound	Source Region			Source Type		
	SCE[b]	ICE	PIE	BB[b]	AN	Mixed
CO (ppb)	101.3 ± 42.8	90 ± 43.3	82.7 ± 19.5	97.5 ± 42.5	111.4 ± 43.2	91.2 ± 41.9
O_3 (ppb)	31.1 ± 15	40.9 ± 21.3	44 ± 22.6	35.1 ± 16.9	29.8 ± 15.3	41.4 ± 16.6
NO_y (ppb)	1.1 ± 1.2	0.7 ± 0.3	0.7 ± 0.2	0.7 ± 0.3	1.2 ± 1.3	1.1 ± 0.8
CH_3COCH_3 (ppt)	603.5 ± 357	1040.3 ± 753	447.1 ± 295	686.3 ± 493.2	632.5 ± 397.2	634.2 ± 302.7
CH_3CN (ppt)	120.3 ± 145	225.3 ± 229	120 ± 63.8	225.3 ± 208.9	84 ± 25	103.8 ± 38.2
C_2H_2 (ppt)	48.4 ± 23.6	117.9	65 ± 13	76 ± 24.8	28.2 ± 3.6	N.A.[b]
C_2H_6 (ppt)	238.3 ± 179	391.8 ± 240.5	304.9 ± 116.2	325.2 ± 203	258.6 ± 176.4	241.9 ± 214.6
C_3H_8 (ppt)	82.8 ± 93.6	69.9 ± 31.2	72 ± 37.8	60.5 ± 37.3	83.9 ± 89.1	96 ± 122.1
i-C_4H_{10} (ppt)	17.9 ± 22.5	9.9 ± 5	7 ± 4.7	7.5 ± 5	17.6 ± 22.6	27.8 ± 32.9
n-C_4H_{10} (ppt)	24 ± 32.7	13.6 ± 5.9	11.1 ± 7.8	11 ± 6.5	23.4 ± 32.8	28.7 ± 38.2
i-C_5H_{12} (ppt)	14.5 ± 17.7	7.1 ± 5.6	5.3 ± 4.4	4.8 ± 5.3	15.5 ± 18.5	14.4 ± 18.6
n-C_5H_{12} (ppt)	9 ± 11.3	3.9 ± 2.1	3.1 ± 3.2	2.7 ± 2.6	7.6 ± 12.4	9.9 ± 10.4
C_6H_6 (ppt)	66 ± 80.1	48.4 ± 31.3	28.4 ± 12.6	32.5 ± 25.4	65.9 ± 70.5	76.9 ± 109.9
$C_6H_5CH_3$ (ppt)	61 ± 73.7	10.3 ± 15.4	2.9 ± 2.9	7 ± 12.6	49.3 ± 60.7	75 ± 127.5
C_2Cl_4 (ppt)	2.5 ± 4.3	0.5 ± 0.4	0.4 ± 0.7	0.4 ± 0.5	2.7 ± 4.6	2.1 ± 3.3
CH_3Cl (ppt)	54.5 ± 37.9	64.9 ± 18.7	34.3 ± 10.7	55.3 ± 25	49.6 ± 30.9	59.5 ± 62.4
TGM[b] (ng/m^3)	0.7 ± 0.3	0.2 ± 0.1	0.3 ± 0.1	0.4 ± 0.2	0.8 ± 0.3	0.3 ± 0.2

[a]Data represent the mean enhancement plus the standard deviation.
[b]SCE, south China events; ICE, Indochinese Peninsula events; PIE, Philippines/Indonesia events; BB, biofuel burning emissions; AN, anthropogenic sources; TGM, total gaseous mercury; N.A., data not available.

anthropogenic emissions and elevated CO from biomass/biofuel burning is difficult because most of the air parcels encountered in Asian outflow represent a mixture of sources having varying contributions. To find out the main contributing source to a certain air parcel during high-CO events, chemical tracers, such as acetonitrile and CH_3Cl for biomass burning and C_2Cl_4 for anthropogenic (urban/industrial) emissions were used to examine the influence of these sources. For those events showing the influence of both source categories, the ratio of ΔTGM/ΔCO (total gaseous mercury), which has been found to be different within anthropogenic (higher value) and biomass/biofuel burning (lower value) plumes [*Slemr et al.*, 2009], was used to further classify the relative strength of both sources. Furthermore, back trajectory analysis for tracing of source regions, fire maps for fire events, and satellite cloud images for convection were also used to confirm the source region and the pathway of CO uplift from surface sources.

[19] Three types of air parcel classifications were used: air parcels impacted primarily by urban/industrial anthropogenic sources (AN air parcels), air parcels with greater biomass and/or biofuel burning emissions (BB air parcels), and air parcels that are a mixture of the two, where a dominant source is unclear. According to our analysis, 17 of the observed high-CO events were BB air parcels, 17 were AN air parcels and the remaining 17 were a mixture of the two. AN air parcels were encountered mainly during the SCEs (16 of 17 high-CO events). BB air parcels were observed in air originating from all regions, although, 7 of 17 BB air parcels were encountered during ICEs. Correla-

Table 2. Correlations Between CO and the Trace Gases of Ozone, Reactive Nitrogen, Acetone, and Acetonitrile During Biomass/Biofuel Burning Events[a]

Date	Region	CO (ppb)	$\Delta O_3/\Delta CO$ (ppb/ppb)	$\Delta NO_y/\Delta CO$ (ppt/ppb)	$\Delta CH_3COCH_3/\Delta CO$ (ppt/ppb)	$\Delta CH_3CN/\Delta CO$ (ppt/ppb)
25 Oct 2007	SC	84.3	N.C.	N.A.	3.74(0.42)	N.C.
27 Apr 2006	IC	55.7	0.41(0.37)	N.C.	6.89(0.37)	N.C.
20 Oct 2006	IC	109.6	N.C.	9.0(0.20)	3.43(0.27)	N.C.
18 Apr 2007	IC	200.3	0.07(0.34)	N.A.	8.27(0.90)	0.93(0.67)
19 Apr 2007	IC	106.5	−0.58(0.93)	N.A.	N.A.	N.A.
19 Apr 2007	IC	82.2	0.47(0.34)	22.9(0.82)	N.A.	N.A.
19 Apr 2007	IC	59.0	N.C.	17.7(0.72)	N.A.	N.A.
19 Apr 2007	IC	84.3	N.A.	10.0(0.65)	N.A.	N.A.
27 Mar 2008	IN	133.9	0.24(0.85)	N.A.	6.37(0.26)	0.71(0.55)
27 Mar 2008	IN	197.1	0.15(0.73)	N.A.	5.47(0.52)	1.25(0.91)
20 Oct 2006	PI	107.5	0.20(0.38)	7.0(0.94)	4.90(0.63)	1.76(0.73)
20 Oct 2006	PI	105.4	N.C.	5.2(0.97)	3.58(0.62)	1.16(0.48)
26 Feb 2008	PI	89.6	0.13(0.82)	N.A.	7.36(0.87)	0.72(0.29)
22 Jun 2007	NEA	72.7	N.A.	N.C.	N.C.	N.C.
08 Sep 2006	SC	69.6	N.A.	19.6(0.56)	N.A.	N.A.
19 Oct 2006	SC	58.0	N.C.	11.1(0.54)	7.89(0.72)	N.C.
20 Oct 2006	SC	63.2	N.C.	N.A.	3.87(0.31)	2.73(0.83)
25 Oct 2007	SC	75.9	N.C.	N.A.	N.C.	N.C.

[a]SC, south China; IC, Indochina; IN, India; PI, Philippines; NEA, northeast Asia; N.C., no correlation; N.A., data not available.

Table 3. Correlations Between CO and the Trace Gases of Ozone, Reactive Nitrogen, Acetone, and Acetonitrile During Anthropogenic Events

Date	Region	CO (ppb)	$\Delta O_3/\Delta CO$ (ppb/ppb)	$\Delta NO_y/\Delta CO$ (ppt/ppb)	$\Delta CH_3COCH_3/\Delta CO$ (ppt/ppb)	$\Delta CH_3CN/\Delta CO$ (ppt/ppb)
14 Dec 2006	PI	73.8	0.19(0.54)	7.4(0.56)	2.28(0.57)	N.C.
19 May 2005	SC	131.8	N.A.	N.A.	N.A.	N.A.
31 Jul 2006	SC	179.2	0.11(0.44)	13.9(0.71)	8.39(0.67)	N.A.
01 Aug 2006	SC	115.9	0.27(0.33)	N.A.	4.93(0.61)	N.C.
08 Sep 2006	SC	120.2	N.A.	3.5(0.76)	N.A.	N.A.
14 Nov 2006	SC	105.4	−0.20(0.36)	N.A.	4.17(0.80)	0.55(0.18)
15 Nov 2006	SC	80.1	−0.11(0.84)	N.A.	N.A.	N.A.
14 Dec 2006	SC	138.1	−0.09(0.68)	3.6(0.30)	N.C.	−0.42(0.21)
22 May 2007	SC	63.2	N.C.	6.4(0.29)	9.70(0.50)	1.23(0.30)
22 May 2007	SC	84.3	N.C.	8.1(0.61)	5.71(0.51)	0.29(0.14)
22 May 2007	SC	52.7	N.C.	15.8(0.55)	6.11(0.64)	N.C.
23 May 2007	SC	105.4	−0.24(0.90)	22.4(0.27)	3.98(0.81)	0.24(0.29)
21 Jun 2007	SC	115.9	−0.2(0.51)	N.C.	4.07(0.44)	N.C.
18 Jul 2007	SC	221.3	N.C.	1.6(0.52)	4.92(0.92)	0.24(0.59)
14 Aug 2007	SC	115.9	N.C.	17.9(0.76)	9.90(0.96)	N.C.
13 Nov 2007	SC	79.1	N.C.	2.3(0.49)	3.54(0.20)	N.C.

tions between CO and the trace gases O_3, NO_y, acetonitrile and acetone from each high-CO event during BB, AN and mixed event types are given in Tables 2–4.

[20] Varying O_3 levels were observed in both BB air parcels and AN air parcels, and in most cases O_3 mixing ratios were enhanced, indicating photochemical processing in the air parcel before interception. During high-CO events, O_3 only infrequently correlated with CO, and good positive correlations (R^2 >0.5) between CO and O_3 were found for only 7 events, accounting for less than 20% of all events. This is likely a result of the inhomogeneous compositions of intercepted air parcels, as they may contain several air parcels from different origin and with different aging features. Positive correlations between O_3 and CO were only found during 3 AN air parcels (R^2 were 0.54, 0.44 and 0.33, respectively). The correlation between O_3 and CO within BB air parcels showed regional differences. Significant positive correlations were not only found in the air parcels from Northeast Asia (1 event, $R^2 = 0.59$) and India (2 events, R^2 were 0.85 and 0.73, respectively) but also found in some of the air parcels from Philippines/Indonesia and Indochinese Peninsula. Significant enhancements of both CO and O_3 were found but no correlations were observed between them in the BB air parcels from south China.

[21] As a unique tracer of BB, acetonitrile was significantly enhanced and the enhancement ranged from ~90–~780 ppt in the BB air parcels although measurements of acetonitrile were not available for some of the BB air parcels. Correlations between CO and acetonitrile were found in 7 BB air parcels with $\Delta CH_3CN/\Delta CO$ ratio ranging from 0.71 to 2.73 ppt/ppb. In the whole data set (12 events), acetonitrile was correlated, albeit weakly ($R^2 = 0.36$), with CO in the BB air parcels, with a slope of 1.10 ppt/ppb. Correlations between CO and acetonitrile were clearly found in the PIEs and INEs (Table 3). Nevertheless, correlation was not observed in 5 BB air parcels from the source regions of Indochinese Peninsula and south China. This may be caused by the complexity of air-parcel composition during transport.

[22] Reactive nitrogen (NO_y), representing the sum of reactive nitrogen species such as NO, NO_2, PAN, HNO_3 etc., can play an important role in photochemistry in the UT [*Fahey et al.*, 1995]. During CARIBIC flights, strong spikes of NO_y are frequently observed, which are attributed to aircraft emissions [*Fahey et al.*, 1995]. After excluding these spikes, enhancements of NO_y were observed in both BB and

Table 4. Correlations Between CO and the Trace Gases of Ozone, Reactive Nitrogen, Acetone, and Acetonitrile During Events of Mixed (Anthropogenic and Biomass/Biofuel Burning) Sources

Date	Region	CO (ppb)	$\Delta O_3/\Delta CO$ (ppb/ppb)	$\Delta NO_y/\Delta CO$ (ppt/ppb)	$\Delta CH_3COCH_3/\Delta CO$ (ppt/ppb)	$\Delta CH_3CN/\Delta CO$ (ppt/ppb)
27 Apr 2006	IC	76.3	0.05(0.47)	N.A.	N.A.	N.A.
28 Apr 2006	IC	73.8	N.C.	N.A.	N.C.	N.C.
30 May 2006	IC	52.7	N.C.	N.C.	17.34(0.79)	1.69(0.23)
15 Nov 2006	PI	74.8	0.48(0.37)			
25 Oct 2007	PI	74.8	0.32(0.53)	N.A.	4.02(0.33)	N.C.
26 Feb 2008	PI	52.7	−1.18(0.94)	N.A.	N.C.	1.04(0.29)
01 Aug 2006	NEA	95.9	0.45(0.59)	13.7(0.21)	7.42(0.85)	N.C.
08 Sep 2006	NEA	171.8	N.A.	N.C.	N.A.	N.A.
27 Apr 2006	SC	73.8	N.A.	N.A.	7.96(0.96)	0.63(0.73)
05 Jul 2006	SC	189.7	0.04(0.27)	3.8(0.54)	4.42(0.56)	N.C.
06 Jul 2006	SC	158.1	N.C.	N.C.	5.49(0.66)	N.C.
01 Aug 2006	SC	56.9	N.C.	N.A.	3.63(0.55)	N.C.
19 Oct 2006	SC	63.2	N.C.	N.A.	6.21(0.66)	N.C.
14 Dec 2006	SC	98.0	0.04(0.29)	2.1(0.28)	2.02(0.38)	N.C.
05 Feb 2007	SC	63.2	N.C.	N.A.	N.C.	0.73(0.94)
15 Aug 2007	SC	98.0	0.24(0.40)	N.C.	6.40(0.78)	0.58(0.27)
15 Aug 2007	SC	76.9	0.39(0.74)	N.A.	2.81(0.53)	N.C.

AN air parcels. The peak value of NO_y varied from ~1.0 ppb to ~4.5 ppb, in some cases reaching ~6–8 ppb in AN air parcels, which is much higher than enhancements of 1–2 ppb encountered in BB air parcels. The average of NO_y enhancement in the AN air parcels was found to be stronger than in BB air parcels (Table 1), showing urban/industrial sources to be a stronger contributor to NO_y. The correlation between NO_y and CO were found in both AN air parcels and BB air parcels with various $\Delta NO_y/\Delta CO$ ratios. In all AN air parcels $\Delta NO_y/\Delta CO$ ratio ranged from 2.3 to 22.4 ppt/ppb. Higher $\Delta NO_y/\Delta CO$ ratios was found for BB air parcels encountered during SCEs (11.1–19.6 ppt/ppb) and ICEs (9.0–22.9 ppt/ppb) than found for PIEs (5.2–7 ppt/ppb).

[23] Enhanced acetone (CH_3COCH_3) was observed during all events, and this was found to be correlated with CO in most of all air parcels. The $\Delta CH_3COCH_3/\Delta CO$ ratio ranged from 2.02 to 17.34 ppt/ppb. This suggests that the production acetone is highly related to other pollutants in the polluted air parcels. According to previous studies, acetone enhancements can be attributed to production during photochemical aging when there is an ample supply of precursors coupled with sufficient conditions for chemical processing [*Singh et al.*, 1994]. No significant difference could be observed between AN air parcels and BB air parcels. In the BB air parcels, no difference between $\Delta CH_3COCH_3/\Delta CO$ ratios could be found among the air parcels influenced by different regions.

[24] As expected, a number of NMHCs and halocarbons were elevated in the whole air samples collected during high-CO events. Over the investigated region, 17 air samples were collected during 16 high-CO events influenced by biomass/biofuel burning, 13 during the 9 influenced by AN air parcels and 4 from four mixed air parcels. Enhancements of trace gases influenced by the different source categories are shown in Table 1. C_2H_6, a relatively long-lived NMHC, was measured with higher enhancements in BB air parcels than in AN air parcels. Given the frequency of open fires and the widespread use of biofuels in the region, biomass/biofuel burning is likely to be a large source for C_2H_6 in Asian outflow, as has been found previously [*Blake et al.*, 2003]. In contrast to C_2H_6, enhancements of shorter-lived species such as C_3H_8, i-C_4H_{10}, n-C_4H_{10}, i-C_5H_{12}, and n-C_5H_{12} were higher in AN air parcels. Because these compounds have much shorter lifetimes in the atmosphere compared to C_2H_6, their enhancements may be the products of shorter transport times associated with frequent convection over south China, where anthropogenic emission is suggested to be the dominant source.

[25] Ethyne (C_2H_2) is a tracer of combustion emitted by both urban/industrial combustion processes, primarily the burning of fossil fuels, and biomass/biofuel burning [*Blake et al.*, 1992; *Blake et al.*, 1993]. In this study, C_2H_2 was only measured in May 2005 and from October 2007 to March 2008 (altogether 19 flights). There were 6 samples collected in the BB air parcels and 2 in AN air parcels, with BB air parcels having larger enhancements of ethyne.

3.3.2. South China Events (SCEs)

[26] Of the 51 high-CO events, 29 (57%) can be classified as SCEs. These were found over south China during FRA ↔ CAN flights and over the Chinese coast during CAN ↔ MNL flights. CO enhancements during these events were accompanied by enhancements of aerosols and trace gases such as acetone, acetonitrile, NO_y, and TGM, however, the species and the magnitude of their enhancements were variable, depending on the source contribution, composition, and evolution of the air parcels.

[27] During the SCEs, indicators of convection have often been observed, as shown by increased water vapor, and frequently by cloud contact of the trajectories within the preceding 48 h when convective clouds were observed. The strong coupling of large CO enhancements with local convection during the SCEs indicates that local sources in south China were dominant. Enhancements of short-lived NMHCs such as propane (C_3H_8), i-butane (i-C_4H_{10}), n-butane (n-C_4H_{10}), i-pentane (i-C_5H_{12}), and n-pentane (n-C_5H_{12}) were also observed, and enhancements during the SCEs were larger than during other events (PIEs and ICEs) (Table 1). Ozone, an indicator of air parcel processing, was also enhanced, but the enhancement was lower than the other regions, suggesting relatively fresh air parcels during the SCEs. The large enhancements in NMHCs and the relatively small O_3 enhancements indicate much shorter transport times for air parcels encountered during SCEs, possibly as a result of fast convective transport of polluted air from the boundary layer. Furthermore, enhancements of short-lived 4–12 nm particles (N_{4-12}) ranged from ~15×10^3 to ~300×10^3 particles cm^{-3}, also indicating that these air parcels were relatively fresh [*Hermann et al.*, 2003]. A previous CARIBIC study of aerosols showed that many strong high-aerosol events (especially in fine particles) are associated with recent boundary layer contributions [*Köppe et al.*, 2009].

[28] The rapid industrialization of south China, encompassing the dynamic Yangtze River Delta region and the Pearl River Delta region, has led to serious air pollution problems in these regions [*Cao et al.*, 2003; *Tang et al.*, 2009]. Large enhancements of tetrachloroethylene (C_2Cl_4) and toluene (C_7H_8) suggest that industrial emissions are important contributors to pollutants during SCEs, in addition to other combustion related sources (Table 1). C_2Cl_4 is used as a solvent and in previous studies has proven itself to be a valuable tracer for the influence of urban/industrial activities on Asian outflow [*Barletta et al.*, 2009]. Toluene, partly emitted from transportation and partly from its use as solvent, is another tracer of urban emissions which was reported to be largely enhanced in south China [*Tang et al.*, 2009].

[29] During those high-CO events where TGM measurements were made, enhancements were also observed in TGM. Because of the low temporal resolution of TGM measurements, correlations of TGM versus CO can only be investigated for 16 SCEs of longer duration. Significant correlations were found during 11 events, 7 of which had slopes >7 pg/m^3 ppb, which is characteristic of anthropogenic emissions [*Slemr et al.*, 2009]. On the basis of the enhancements of anthropogenic tracers, 17 of 29 SCEs were found to be influenced mainly by anthropogenic emissions.

[30] During the SCEs, the enhancement of NO_y was much higher compared to that for the other two regions. The largest enhancements in NO_y were observed during events having the largest enhancements in urban/industrial tracers such as toluene and C_2Cl_4, with the highest NO_y enhancement reaching ~6 ppb. This shows that urban/industrial sources also had a strong influence on NO_y [*Singh et al.*, 1996].

[31] The strongest high-CO event was encountered on 18 July 2007 over south China (FRA → CAN) (Figure 3). The event started at 06:49 UTC (local time 14:49) and ended at 07:06 UTC (local time 15:06), lasting for ~17 min

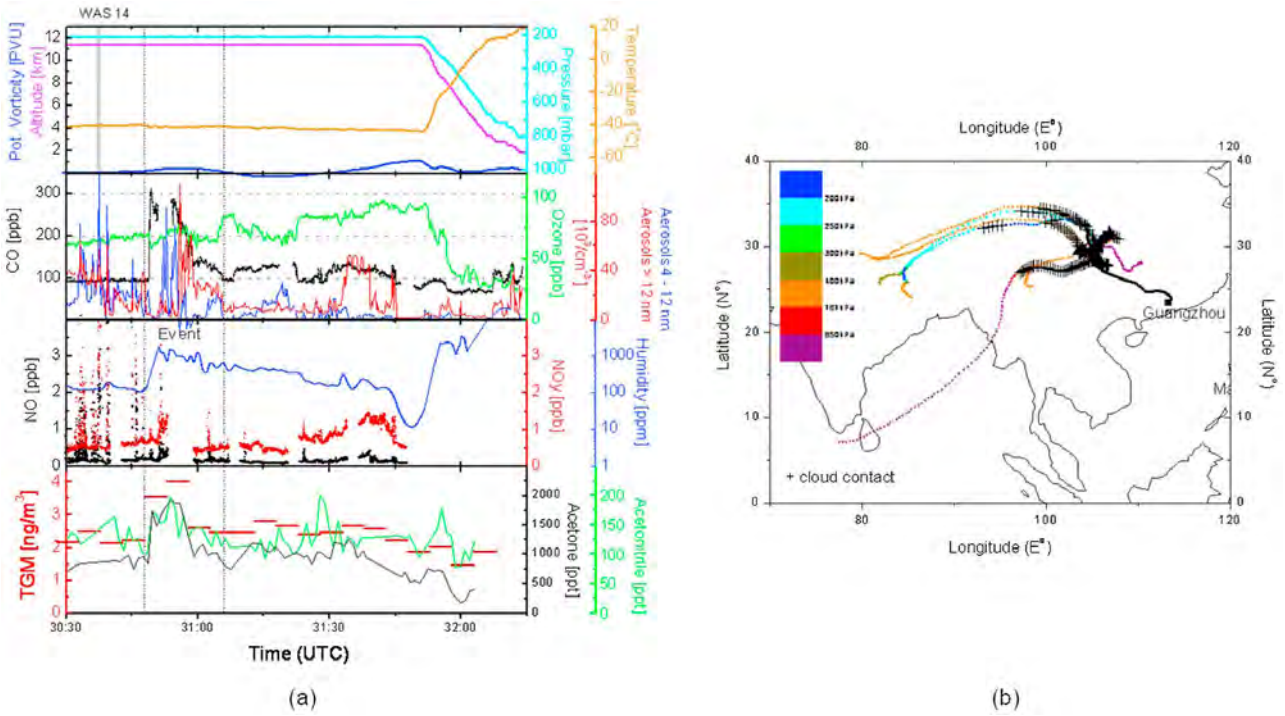

Figure 3. South China event on 17 July 2007: (a) data overview and (b) 5 d back trajectories (dotted lines) and 2 d cloud contact analysis (crosses). Trajectories are color coded by pressure. In Figure 3a, panels from top to bottom are potential vorticity, flight altitude, CO and whole air sampling intervals (gray bars; labeled "WAS"); O_3, NO_y, N_{4-12}, and N_{12}; and total gaseous mercury (TGM), acetone and acetonitrile.

at a constant cruising altitude of ~11.5 km. The peak CO value was 321.5 ppb, ~221.3 ppb above the background level. The CO enhancement was accompanied by elevated mixing ratios of O_3 (60–80 ppb) and NO_y (from ~0.5 to ~1.5 ppb), TGM (from ~2 to ~4 ng/m^3), acetone (from ~850 to ~1930 ppt) and acetonitrile (from ~120 to ~200 ppt) (Figure 3a), however no whole air samples happened to have been collected during this event.

[32] According to the back trajectories, 2 d prior the air parcels had been advected through the free troposphere (~2–5.5 km) and the planetary boundary layer (<2 km) over south China. Strong increases in water vapor (from ~150 to ~600 ppm) indicate convective processes, and convection is further confirmed by convective cloud shown in cloud image and also by cloud contact analysis. The cloud contact analysis which shows that most of the back trajectories during this event had been in contact with clouds over south China in the previous 48 h (Figure 3b). The presence of convection implicates local sources during the events. The position of the aircraft during this high-CO event ranged from 29.5°N, 104.9°E to 27.4°N, 106.0°E, over the provinces of Sichuan and Guizhou. Coal power plants and metal smelting are the major type of industries in these two provinces increasing the likelihood of industrial emissions being the major source in this case.

[33] To investigate the contribution of different source categories, correlations with CO were analyzed. Ozone was slightly enhanced but had no correlation with CO during the event, giving an indication that the observed air parcels were relatively fresh. Nevertheless, acetone, which results from primary emission and/or secondary formation [*Singh et al.*, 1994], had a good correlation with CO (R^2 = 0.92; slope, 5.18 ppt/ppb). During a previous airborne campaign in the region, $\Delta CH_3COCH_3/\Delta CO$ was reported as 3.0 ppt/ppb in a south China plume of anthropogenic emissions in the free troposphere (5–10 km) [*Singh et al.*, 1995], which is lower than during the CARIBIC event.

[34] Significant correlations were found between CO and NO_y (R^2 = 0.52), CH_3CN (R^2 = 0.59), and TGM (R^2 = 0.96). The $\Delta TGM/\Delta CO$ ratio of 11.4 pg/m^3 ppb is higher than those obtained in earlier studies of Asian and European outflow [*Jaffe et al.*, 2005; *Slemr et al.*, 2006], indicating a strong influence of local industrial emissions. As stated above, many coal-fired power plants are located in the provinces Guizhou and Sichuan [*Jiang et al.*, 2006; *Wu et al.*, 2010] and mercury and artisanal gold mining are located in Guizhou [*Wang et al.*, 2007]. However, enhanced acetonitrile and its correlation with CO indicate that BB also contributed to the CO increase. Indeed, previous results show that Asian outflow contains a mixture of anthropogenic and biomass burning emissions [*Russo et al.*, 2003]. The emission ratio of $\Delta CH_3CN/\Delta CO$ was 0.24 ppt/ppb, much lower than the ratio of ~1.73 ppt/ppb from fresh tropical forest fires [*Andreae and Merlet*, 2001], indicating that BB was not as important as industrial emissions. Additionally, MODIS fire counts show almost no open fires in the regions over which air parcel back trajectories had passed. Biofuel burning, common in southern China and the Indochinese Peninsula [*Streets et al.*, 2003] is therefore the likely source contributing to the CO enhancement.

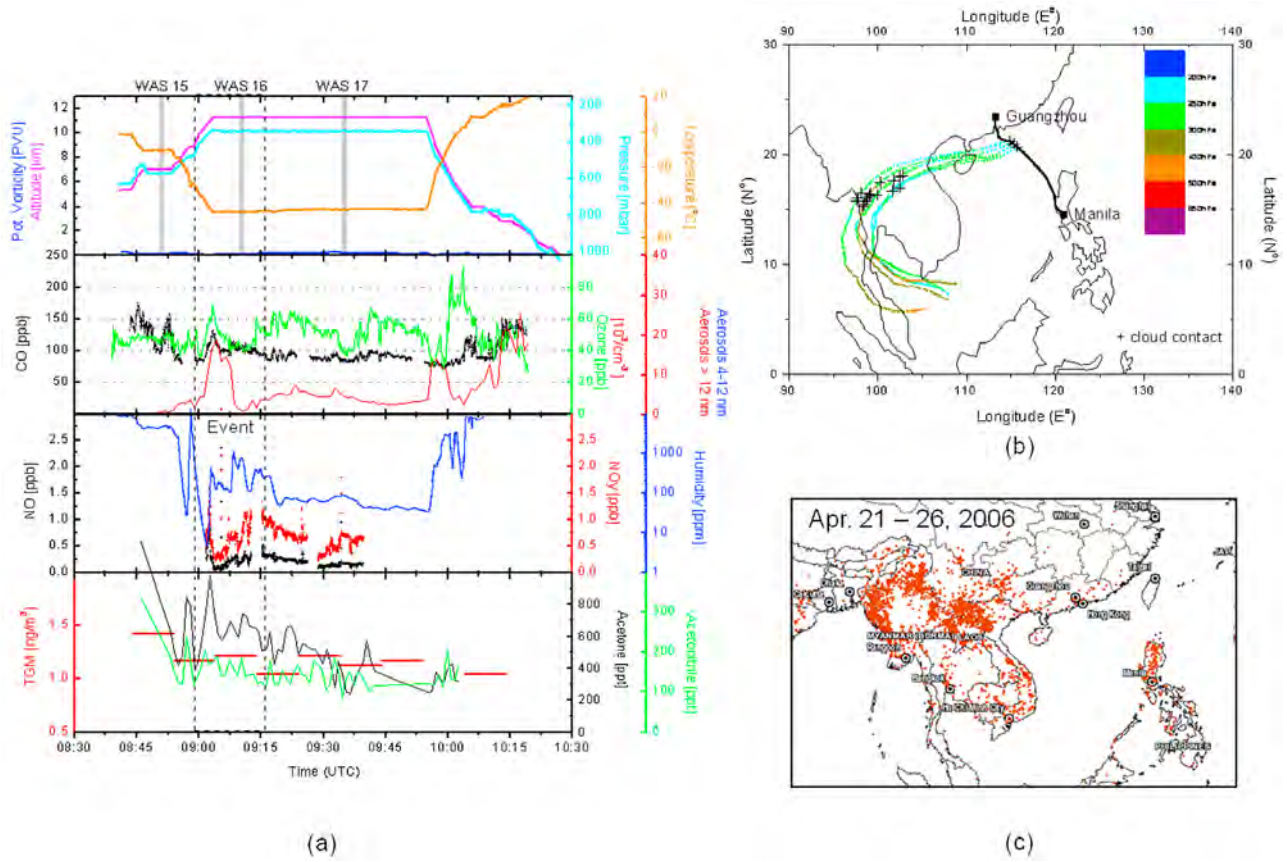

Figure 4. Indochinese Peninsula event on 28 April 2006: (a) data overview (for panel information please refer to Figure 3a); (b) 5 d back trajectories (dotted lines) and 2 d cloud contact analysis (crosses); and (c) satellite map of fire spots from the Fire Information for Resource Management System (FIRMS) web fire mapper based on the Moderate Resolution Imaging Spectroradiometer (MODIS) detection (http://firefly.geog.umd.edu/firemap/). In Figure 4b trajectories are color coded by pressure.

3.3.3. Indochinese Peninsula Events (ICEs)

[35] Ten high-CO events originated from the Indochinese Peninsula (ICE). However, the actual CO enhancements were not as large as during SCEs: except for one event that reached ~190 ppb CO, values were between ~50 and ~115 ppb. Concomitant enhancements of O_3, NO_y, acetone, acetonitrile and aerosols were also observed. Acetonitrile mixing ratios were higher during the ICEs (Table 1), indicating the strong influence of BB. Levels of another BB tracer, CH_3Cl (measured from the whole air samples), were also higher during ICEs than during events from other regions. Strong increase in O_3 and acetone were also observed, pointing to the photochemical aging of air parcels during transport from the source region. N_{12} aerosol concentrations were elevated, more so than N_{4-12} which were only slightly elevated, and lower concentrations of short-lived fine particles also suggest a substantial degree of photochemical aging. Compared to the SCEs, stronger enhancements of ethane and weaker enhancements of short-lived hydrocarbons were observed in the whole air samples. Mixing ratios of toluene and C_2Cl_4 were also elevated, showing some influence of urban/industrial emissions, although enhancements were not as large as during SCEs. On average, TGM was lowest during ICEs and much lower than during SCEs, another indication of the reduced influence of urban/industrial emissions from this region relative to south China. Enhancements of NO_y during the ICEs were smaller than during the SCEs, but comparable with PIEs (see section 3.3.4).

[36] During previous Asian outflow research campaigns, the Indochinese Peninsula has been frequently reported as a region where BB is responsible for a substantial fraction of total emissions [*Streets et al.*, 2003; *Woo et al.*, 2003]. Agricultural and forest fires are the major open fire types in the dry season (October – March) [*Christopher and Kimberly*, 1996]. Moreover, domestic biofuel burning in this region is also known as a source of CO and BB related atmospheric species [*Streets et al.*, 2003]. The ICEs in our study were observed exclusively in April (2006 and 2007) and October (2006 and 2007), which is in accordance with the seasonality of BB reported in previous studies [*Streets et al.*, 2003]. Seven of the ICEs were found to be related to BB, indicating that it is the most important source of CO enhancements during ICEs. However, distinguishing between biomass burning and biofuel burning is difficult as the products are often the same, albeit in different ratios at emission [*Woo et al.*, 2003].

[37] A case study of typical CARIBIC ICEs was published recently [*Lai et al.*, 2010] showing the influence of BB and a pathway for air parcel transport from the Indo-

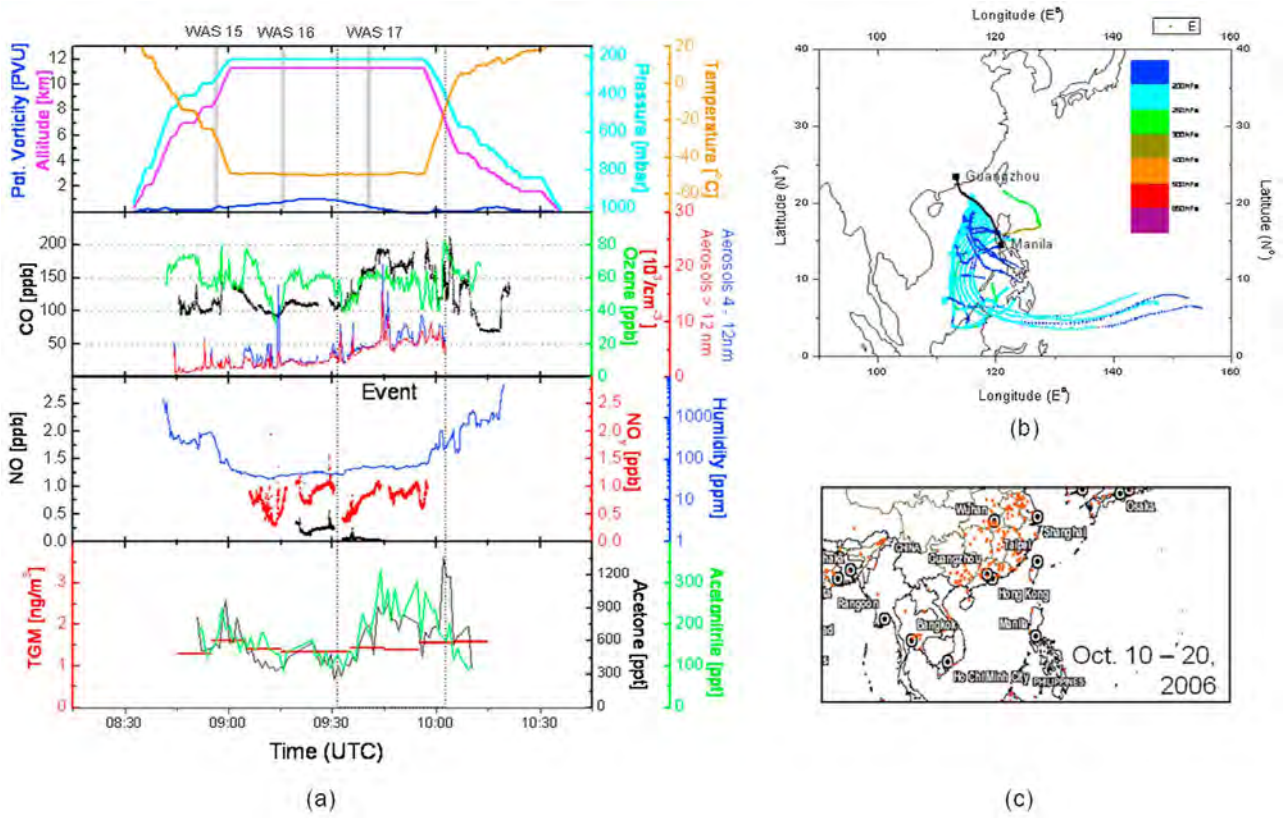

Figure 5. Philippines/Indonesia event on 20 October 2006: (a) data overview (for panel information please refer to Figure 3a); (b) 5 d back trajectories (dotted lines); and (c) satellite map of fire spots from the FIRMS web fire mapper based on the MODIS detection (http://firefly.geog.umd.edu/firemap/). In Figure 5b trajectories are color coded by pressure.

chinese Peninsula. Here we show an additional ICE during a CAN → MNL flight on 28 April 2006 (Figure 4). The high-CO event was encountered at UTC 09:01–09:17 with CO enhanced from a background of ~85 ppb to levels of ~140ppb, O_3 from ~40 to ~65 ppt, NO_y from ~300 to ~1000 ppt, N_{12} from ~4×10^3 to ~20×10^3 particles/cm^3, acetone from ~400 ppt to ~1000 ppt, and acetonitrile from ~140 to ~200 ppt (Figure 4a). Back trajectories point to the Indochinese Peninsula as the source region 2–3 d before encounter. Figures 4b and 4c show that numerous fire spots were observed in this region which, by the enhancement of acetonitrile and its correlation with CO (R^2 = 0.58), implicates BB as the dominant source.

[38] Ozone and acetone are both produced photochemically during transport of air parcels containing their precursors [*Jost et al.*, 2003; *Singh et al.*, 1994]. During the flight on 28 April 2006, both compounds were strongly correlated with CO, with R^2 value of 0.84 and 0.67 for O_3 and acetone, respectively. $\Delta O_3/\Delta CO$ was 0.53 ppb/ppb, which is in the range of values obtained from the other ICEs in April 2007 (0.4–0.9) [*Lai et al.*, 2010] and these ratios are similar to those found for aged plumes (2–6 d aged) [*Andreae et al.*, 2001; *Mauzerall et al.*, 1998]. The slope of $\Delta CH_3COCH_3/\Delta CO$ was 6.89 ppt/ppb, higher than in fresh BB plumes (2.1–4.6 ppt/ppb) [*Andreae and Merlet*, 2001]. The $\Delta O_3/\Delta CO$ and $\Delta CH_3COCH_3/\Delta CO$ ratios indicate that the air parcel probed within the high-CO event was aged, in agreement with low N_{4-12} aerosol concentrations.

[39] Satellite cloud images from 25–26 April, 2–3 d prior to our observations, indicate the occurrence of strong convection in the source area and our cloud contact analysis shows that the air parcel had been in contact with clouds in the preceding 48 h. The combination of all these indicators shows that CO and other chemical species produced by open fires were uplifted by convective processes to the UT, where the resulting air parcels after mixing with background air were intercepted during the CARIBIC flight. Forward trajectories show that the air parcels from the Indochinese Peninsula can be further advected to the Pacific Ocean. This pathway might be important for long-range transport of CO and other pollutants from the Indochinese Peninsula via the East Asian Continent to the UT over the Pacific Ocean, which is in agreement with previous studies [*Park et al.*, 2009, 2008].

3.3.4. Philippines/Indonesia Events (PIEs)

[40] The region of the Philippines and Indonesia was the third major source region for the high-CO events, and 7 events are classified as Philippines/Indonesia Events (PIEs). PIEs were encountered over the South China Sea, particularly when flying near the Philippine coast during CAN ↔ MNL flights. The CO enhancements during the PIEs ranged from ~50 to ~110 ppb and the largest CO enhancement was not as high as those during SCEs and ICEs. Concomitant enhancements were also observed for other trace gases, such

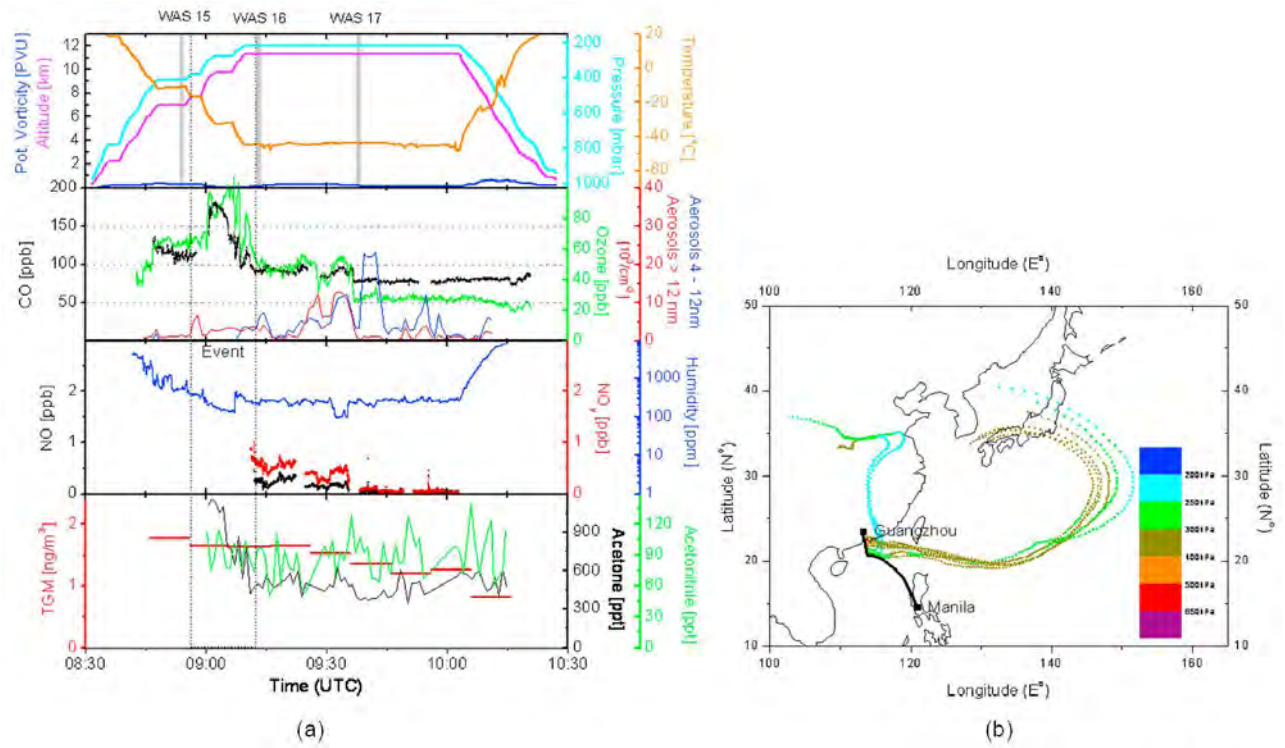

Figure 6. Northeast Asia event on 1 August 2006: (a) data overview (for panel information please refer to Figure 3a) and (b) 5 d back trajectories (dotted lines), color coded by altitude.

as acetone, acetonitrile, TGM, and aerosols, depending on sources influencing each event. The influence of BB was evident from the enhancement of acetonitrile, which was lower than during ICEs and similar to enhancements during SCEs. Three PIEs were found to be related to BB. Furthermore, the largest enhancement of O_3 and the smallest enhancements of NO_y and acetone were observed during the PIEs. The results of measurements of whole air samples show that mixing ratios of ethyne and ethane were lower than during the ICEs but higher than during the SCEs. Mixing ratios of short-lived NMHCs were similar to levels during the ICEs and much lower than during the SCEs. Benzene, toluene and C_2Cl_4 had the lowest mixing ratios during PIEs, which may be related to less dense local population and industry.

[41] A typical PIE observed during the flight in October 2006 is shown in Figure 5. A distinct CO enhancement (from ~100 to ~210 ppb) was measured with a duration of more than 1 h (from 09:30 UTC to 10:13 UTC). The event was encountered at a cruising altitude of ~11.3 km on the route to MNL and lasted until descent. It is one of several long-duration events found during the flights. During the event, O_3 increased from ~40 to ~80 ppb, acetonitrile from ~95 to ~330 ppt, acetone from ~280 to ~950 ppt, NO_y from ~400 to ~1000 ppt, N_{4-12} from ~3.0 × 10^3 to ~22 × 10^3 particles/cm^3 STP, and N_{12} from ~2.5 × 10^3 to ~16 × 10^3 particles/cm^3 STP. The strong enhancement of fine particles (N_{4-12}) during this event indicates active particle formation in contrast to aged air. At the beginning of the event, O_3 was only slightly enhanced from ~40 to ~60 ppb, and later increased to ~80 ppb when the aircraft was descending. Hardly any correlation between CO and O_3 (R^2 = 0.20) was observed. Acetonitrile was strongly enhanced and correlated well with CO (R^2 = 0.73) with $\Delta CH_3CN/\Delta CO$ of 1.76 (ppt/ppb), which is similar to that attributed to fresh biomass burning plumes [*Andreae and Merlet*, 2001]. One whole air sample was collected during this event. The analysis of halocarbons showed that CH_3Cl was 670 ppt, which is considerably above the two prior (nonevent) samples (606 ppt and 615 ppt). NMHCs were all highly enhanced, while a lower concentration of the urban/industrial tracer of C_2Cl_4 was also observed (1.8 ppt). These results show BB to have been the major source contributing to the high-CO event.

[42] Back trajectories during this event indicate that the air parcels were transported through the UT over the region of the Philippines/Indonesia, which we believe had a strong influence on composition (Figure 5b). Before and during the sampling period (Figure 5c), large forest fires occurred at many sites in Indonesia, south of our observation. Satellite borne measurement of CO shows that elevated CO had spread over Indonesia and the adjacent regions during that period. After and during long periods of burning in Indonesian forests, CO produced not only filled the lower-altitude atmosphere (PBL and FT) but also intruded into the UT. With air from the UT over this region, CO was transported to the CARIBIC observation point. Therefore, the Indonesian forest fires at that time are identified as the major contributor to this specific PIE.

3.3.5. Long-Range Transport: Northeast Asia Events (NEAEs) and India Events (INEs)

[43] Back trajectory analyses show that 5 of the 51 high-CO events were the result of longer-range transport from regions other than those previously discussed. Three events were attributed to transport from northeast Asia (NEA,

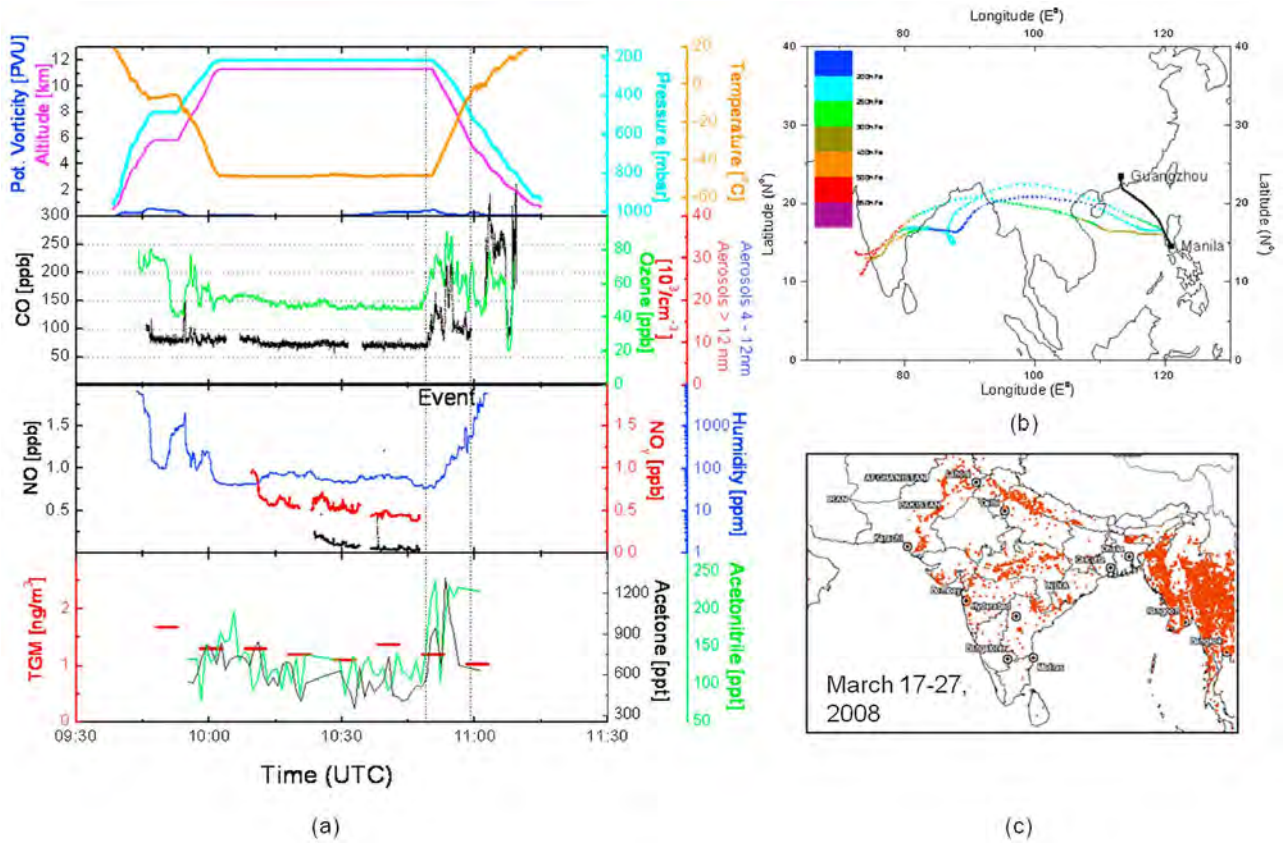

Figure 7. India event in March 2008: (a) data overview (for panel information please refer to Figure 3a); (b) 5 d back trajectories (dotted lines); and (c) satellite map of fire spots from the FIRMS web fire mapper based on the MODIS detection (http://firefly.geog.umd.edu/firemap/). In Figure 7b trajectories are color coded by pressure.

including North China, Korea and Japan) while the back trajectories of two high-CO events were found to have had passed over India (IN). All of these events were observed over the South China Sea on flights between Guangzhou and Manila.

[44] During these 5 events, the most prominent feature was strong enhancements of O_3, which was well correlated with CO (R^2 = 0.59–0.85). These strong enhancements in O_3 indicate considerable photochemical processing having taken place during transport from the respective source regions, which could have taken 5 to 10 d, according to the back trajectories.

[45] The northeast Asia events (NEAEs) were observed during June, August and September. Air parcels originating from Northeast Asia passed over the Western Pacific Ocean or the coast and then arrived at the sampling location. A similar pattern for O_3 transport has been reported by previous studies [*Li et al.*, 2001; *Liu et al.*, 2002]. During the summer months, convection is frequently observed in Northeast Asia [*Qian and Lee*, 2000]. Meanwhile, the UT over East Asia was influenced by the Tibetan anticyclone, under which a large fraction of uplifted air circulates southward and then westward. Contributions of local emissions (anthropogenic emissions and BB) and oceanic emissions were observed during the NEAEs [*Liu et al.*, 2002; *Park et al.*, 2008].

[46] A typical case of a NEAE was observed during a CAN → MNL flight in August 2006 (Figure 6). During ascent from Guangzhou, increased CO was observed at an altitude range of 7.6–11.3 km from 08:48–09:12 UTC. The peak mixing ratio of CO was 179.6 ppb at ~9.8 km, representing ~95 ppb enhancement over the background level. The concurrent O_3 mixing ratio was enhanced from a background of ~60 ppb to ~100 ppb and it correlated well with CO (R^2 = 0.68), indicating photochemical processing. Enhanced acetone was also observed, having a very good correlation with CO (R^2 = 0.85). The slope of $\Delta CH_3COCH_3/\Delta CO$ was 7.41 ppt/ppb, which is close to typical values obtained for aged air parcels (0.5–7 d) [*Mauzerall et al.*, 1998]. Northeast Asia is a highly populated region with dense urban areas including several megacities, such as Beijing, Seoul and Tokyo, and vast industrial areas. The contributions of anthropogenic and BB sources in this region have been widely reported [*Blake et al.*, 2003; *Russo et al.*, 2003]. During transport, the sufficient supply of NMHCs from source regions and long transport times may favor acetone formation. In this particular case, the acetontrile mixing ratio of ~90 ppt was at background levels indicating a negligible contribution of emissions from BB. Back trajectories show that the air parcels during the NEAEs originated from the FT over North China and Japan ~5 d prior to their interception (Figure 6b).

[47] India is another rapidly developing region in Asia with large and increasing emissions from both anthropogenic and BB sources [*Streets et al.*, 2003]. Two Indian Events (INEs) were observed in March 2008 during the two CAN ↔ MNL flights. During the CAN → MNL flight, a short high-CO event (duration of 7 min) was observed starting at 10:49 UTC and ending at 10:56 UTC (Figure 7a). The peak CO mixing ratio was ~210 ppb, ~130 ppb over the background. This event occurred during descent at an altitude of ~9 km. Back trajectories show that the air parcel had undergone long-range transport, starting from the FT over central India ~4–5 d prior to its interception, traveling across the Indochinese Peninsula in the UT and arriving at the aircraft (Figure 7b). Coincident enhancements of O_3 were also observed from ~50 ppb to ~90 ppb. The correlation between CO and O_3 was very good ($R^2 = 0.85$), which is a further indication of photochemical aging during transport. The event was further characterized by enhancements of N_{12} from ~1.0×10^3 to ~15×10^3 particles/cm^3 STP, acetone from ~500 ppt to ~1300 ppt and acetonitrile from ~100 to ~250 ppt. The strong enhancement of acetonitrile documents the influence of BB, which is supported by the fire maps based on the NASA MODIS measurements showing many fire spots in large parts of India (Figure 7c). Central India, the suggested source region, had abundant fire counts, indicating open biomass burning was the most important source in this case, rather than biofuel burning. Furthermore, a significant correlation between CO and N_{12} was also found ($R^2 = 0.69$). N_{12} includes the aerosols in coagulation mode and accumulation mode which were likely to be produced during plume evolution. The back trajectories had also passed over the Indochinese Peninsula as mentioned, where even more abundant open fires were observed, but the influence from this region seems to be smaller. First, the air passing across the Indochinese Peninsula was through the UT (>11.5 km), with less local influence, since no evidence for convection was observed. Second, a part of the backward trajectories for the event passed across the Indochinese Peninsula but without causing any additional CO enhancement, suggesting that the biomass burning in the Indochinese Peninsula did not impact the source sampled air parcel during this INE.

4. Conclusions

[48] Events with high-CO mixing ratios in the UT observed during CARIBIC flights conducted from 2005 to 2008 over the region between south China and the Philippines were analyzed. Altogether 132 such events were identified during 81 flights, of which 51 events with enhancements larger than 50 ppb were identified and classified as high-CO events. Using back trajectories the high-CO events were subsequently classified according to the different source regions: south China (SCEs), the Indochinese Peninsula (ICEs), the Philippines/Indonesia (PIEs), northeast Asia and India (NEAEs). In nearly all cases the source region could be unambiguously identified. The influences of anthropogenic urban/industrial emissions and biomass/biofuel burning during high-CO events attributed to certain source regions were also investigated. Enhancements of NO_y, TGM, toluene and C_2Cl_4 were larger in AN air parcels compared to BB air parcels. ΔTGM/ΔCO proved to be a useful tool for source identification in Asian outflow; higher-ΔTGM/ΔCO ratios indicate a larger contribution from anthropogenic emissions, while lower ratios are indicative of biomass/biofuel burning. Elevated ΔTGM/ΔCO ratios were mainly observed during the SCEs, suggesting south China to have been an important source region of mercury. Acetonitrile, ethane and ethyne were found to be highly enhanced in the BB air parcels. The regional differences were observed in the relationship of NO_y versus CO and acetone versus CO in the BB air parcels, which may be related to the different burning features from the individual source regions.

[49] The detailed chemical composition of air parcels enabled further classification according to the emission processes responsible for the high-CO mixing ratios and also provided qualitative information about transport times. The majority of high-CO events originated in south China and could be attributed mainly to urban/industrial sources in this region. Prior to and during these events, CO and other pollutants were frequently uplifted by convective processes in the region and the observed chemical signature suggests that the intersected air parcels were relatively fresh. The Indochinese Peninsula was another major source region. The events from this source region had large contributions of CO from biomass/biofuel burning. The chemical signatures of air parcels point to a substantial degree of photochemical processing during transport. Influence of local sources, either anthropogenic or biomass/biofuel burning from Philippines/Indonesia, was also identified. However, Philippines/Indonesia events were less frequent and the CO enhancements were weaker compared to those influenced by south China and the Indochinese Peninsula. CO enhancements influenced by long-range transport from the broad regions of Northeast Asia and India were also observed. The most prominent feature of these events is large enhancements of O_3 and acetone, which corresponds to a large degree of photochemical processing during transport.

[50] The frequency with which these high-CO events were encountered during CARIBIC flights shows that Asian emissions have a significant influence on the composition of not only the lower and free troposphere, but also the upper troposphere over the South China Sea. In light of the rapid growth in regional industries and economies it is possible that enhancements of CO and other trace species during similar, future events will be even larger, which has implications not only regionally, but for those regions to which these air parcels are eventually transported.

[51] **Acknowledgments.** The authors thank Lufthansa Airlines and Lufthansa Technik for their commitment and support. We would also like to thank all members of the CARIBIC team, particularly Andreas Weigelt and Marcus Hermann for development of the cloud contact analysis. The authors finally would like to thank the editor and the three anonymous reviewers for their comments. The development and operation of the CARIBIC system has been financially supported by the German Ministry of Education and Science (AFO 2000), by the European Commission through the GEOmon (Global Earth Observation and Monitoring) Integrated Project under the sixth Framework Program (contract FP6-2005-Global-4-036677), and by grants from Fraport AG and the Max Planck Society. Data are available upon request; please visit www.caribic-atmospheric.com for more information.

References

Andreae, M. O., and P. Merlet (2001), Emission of trace gases and aerosols from biomass burning, *Global Biogeochem. Cycles*, *15*(4), 955–966, doi:10.1029/2000GB001382.

Andreae, M. O., et al. (2001), Transport of biomass burning smoke to the upper troposphere by deep convection in the equatorial region, *Geophys. Res. Lett.*, *28*(6), 951–954, doi:10.1029/2000GL012391.

Baker, A. K., F. Slemr, and C. A. M. Brenninkmeijer (2010), Analysis of non-methane hydrocarbons in air samples collected aboard the CARIBIC passenger aircraft, *Atmos. Meas. Tech.*, *3*(1), 311–321, doi:10.5194/amt-3-311-2010.

Barletta, B., et al. (2009), Characterization of volatile organic compounds (VOCs) in Asian and north American pollution plumes during INTEX-B: Identification of specific Chinese air mass tracers, *Atmos. Chem. Phys.*, *9*(14), 5371–5388, doi:10.5194/acp-9-5371-2009.

Bergamaschi, P., R. Hein, M. Heimann, and P. J. Crutzen (2000), Inverse modeling of the global CO cycle 1. Inversion of CO mixing ratios, *J. Geophys. Res.*, *105*(D2), 1909–1927, doi:10.1029/1999JD900818.

Blake, D. R., D. F. Hurst, T. W. Smith, W. J. Whipple, T.-Y. Chen, N. J. Blake, and F. Sherwood Rowland (1992), Summertime measurements of selected nonmethane hydrocarbons in the Arctic and Subarctic during the 1988 Arctic Boundary Layer Expedition (ABLE 3A), *J. Geophys. Res.*, *97*(D15), 16,559–16,588.

Blake, N. J., S. A. Penkett, K. C. Clemitshaw, P. Anwyl, P. Lightman, A. R. W. Marsh, and G. Butcher (1993), Estimates of atmospheric hydroxyl radical concentrations from the observed decay of many reactive hydrocarbons in well-defined urban plumes, *J. Geophys. Res.*, *98*(D2), 2851–2864, doi:10.1029/92JD02161.

Blake, N. J., et al. (2003), NMHCs and halocarbons in Asian continental outflow during the Transport and Chemical Evolution over the Pacific (TRACE-P) Field Campaign: Comparison with PEM-West B, *J. Geophys. Res.*, *108*(D20), 8806, doi:10.1029/2002JD003367.

Brenninkmeijer, C. A. M., T. Röckmann, M. Bräunlich, P. Jöckel, and P. Bergamaschi (1999), Review of progress in isotope studies of atmospheric carbon monoxide, *Chemosphere Global Change Sci.*, *1*, 33–52, doi:10.1016/S1465-9972(99)00018-5.

Brenninkmeijer, C. A. M., et al. (2007), Civil Aircraft for the Regular Investigation of the Atmosphere Based on an Instrumented Container: The new CARIBIC system, *Atmos. Chem. Phys.*, *7*, 4953–4976, doi:10.5194/acp-7-4953-2007.

Brioude, J., J. P. Cammas, O. R. Cooper, and P. Nedelec (2008), Characterization of the composition, structure, and seasonal variation of the mixing layer above the extratropical tropopause as revealed by MOZAIC measurements, *J. Geophys. Res.*, *114*, D00B01, doi:10.1029/2007JD009184.

Cao, J. J., S. C. Lee, K. F. Ho, X. Y. Zhang, S. C. Zou, K. Fung, J. C. Chow, and J. G. Watson (2003), Characteristics of carbonaceous aerosol in Pearl River Delta Region, China during 2001 winter period, *Atmos. Environ.*, *37*(11), 1451–1460, doi:10.1016/S1352-2310(02)01002-6.

Christopher, D. E., and E. B. Kimberly (1996), *Global Biomass Burning*, 663–670 pp., MIT Press, Cambridge, Mass.

Deeter, M. N., et al. (2003), Operational carbon monoxide retrieval algorithm and selected results for the MOPITT instrument, *J. Geophys. Res.*, *108*(D14), 4399, doi:10.1029/2002JD003186.

Fahey, D. W., et al. (1995), In situ observations in aircraft exhaust plumes in the lower stratosphere at midlatitudes, *J. Geophys. Res.*, *100*(D2), 3065–3074, doi:10.1029/94JD02298.

Global Atmosphere Watch (2010), Guidelines for the measurement of atmospheric carbon monoxide, *GAW Rep. 192*, 51 pp., Geneva, Switzerland.

Heald, C. L., et al. (2003), Asian outflow and trans-Pacific transport of carbon monoxide and ozone pollution: An integrated satellite, aircraft, and model perspective, *J. Geophys. Res.*, *108*(D24), 4804, doi:10.1029/2003JD003507.

Hermann, M., J. Heintzenberg, A. Wiedensohler, A. Zahn, G. Heinrich, and C. A. M. Brenninkmeijer (2003), Meridional distributions of aerosol particle number concentrations in the upper troposphere and lower stratosphere obtained by Civil Aircraft for Regular Investigation of the Atmosphere Based on an Instrument Container (CARIBIC) flights, *J. Geophys. Res.*, *108*(D3), 4114, doi:10.1029/2001JD001077.

Jaffe, D., E. Prestbo, P. Swartzendruber, P. Weiss-Penzias, S. Kato, A. Takami, S. Hatakeyama, and Y. Kajii (2005), Export of atmospheric mercury from Asia, *Atmos. Environ.*, *39*(17), 3029–3038, doi:10.1016/j.atmosenv.2005.01.030.

Jiang, G. B., J. B. Shi, and X. B. Feng (2006), Mercury pollution in China, *Environ. Sci. Technol.*, *40*(12), 3672–3678, doi:10.1021/es062707c.

Jost, C., J. Trentmann, D. Sprung, M. O. Andreae, J. B. McQuaid, and H. Barjat (2003), Trace gas chemistry in a young biomass burning plume over Namibia: Observations and model simulations, *J. Geophys. Res.*, *108*(D13), 8482, doi:10.1029/2002JD002431.

Köppe, M., et al. (2009), Origin of aerosol particles in the mid-latitude and subtropical upper troposphere and lowermost stratosphere from cluster analysis of CARIBIC data, *Atmos. Chem. Phys.*, *9*(21), 8413–8430, doi:10.5194/acp-9-8413-2009.

Lai, S. C., et al. (2010), Pollution events observed during CARIBIC flights in the upper troposphere between South China and the Philippines, *Atmos. Chem. Phys.*, *10*(4), 1649–1660, doi:10.5194/acp-10-1649-2010.

Li, Q. B., et al. (2001), A tropospheric ozone maximum over the Middle East, *Geophys. Res. Lett.*, *28*(17), 3235–3238, doi:10.1029/2001GL013134.

Liu, H. Y., D. J. Jacob, L. Y. Chan, S. J. Oltmans, I. Bey, R. M. Yantosca, J. M. Harris, B. N. Duncan, and R. V. Martin (2002), Sources of tropospheric ozone along the Asian Pacific Rim: An analysis of ozonesonde observations, *J. Geophys. Res.*, *107*(D21), 4573, doi:10.1029/2001JD002005.

Logan, J. A., M. J. Prather, S. C. Wofsy, and M. B. Mcelroy (1981), Tropospheric chemistry: A global perspective, *J. Geophys. Res.*, *86*(C8), 7210–7254.

Matsueda, H., and H. Y. Inoue (1999), Aircraft measurements of trace gases between Japan and Singapore in October of 1993, 1996, and 1997, *Geophys. Res. Lett.*, *26*(16), 2413–2416, doi:10.1029/1999GL900089.

Mauzerall, D. L., J. A. Logan, D. J. Jacob, B. E. Anderson, D. R. Blake, J. D. Bradshaw, B. Heikes, G. W. Sachse, H. Singh, and B. Talbot (1998), Photochemistry in biomass burning plumes and implications for tropospheric ozone over the tropical South Atlantic, *J. Geophys. Res.*, *103*(D7), 8401–8423.

Mühle, J., C. A. M. Brenninkmeijer, T. S. Rhee, F. Slemr, D. E. Oram, S. A. Penkett, and A. Zahn (2002), Biomass burning and fossil fuel signatures in the upper troposphere observed during a CARIBIC flight from Namibia to Germany, *Geophys. Res. Lett.*, *29*(19), 1910, doi:10.1029/2002GL015764.

Nedelec, P., V. Thouret, J. Brioude, B. Sauvage, J. P. Cammas, and A. Stohl (2005), Extreme CO concentrations in the upper troposphere over northeast Asia in June 2003 from the in situ MOZAIC aircraft data, *Geophys. Res. Lett.*, *32*(14), L14807, doi:10.1029/2005GL023141.

Newell, R. E., V. Thouret, J. Y. N. Cho, P. Stoller, A. Marenco, and H. G. Smit (1999), Ubiquity of quasi-horizontal layers in the troposphere, *Nature*, *398*(6725), 316–319, doi:10.1038/18642.

Novelli, P. C. (1999), CO in the atmosphere: Measurement techniques and related issues, *Chemosphere Global Change Sci.*, *1*(1–3), 115–126, doi:10.1016/S1465-9972(99)00013-6.

Novelli, P. C., L. P. Steele, and P. P. Tans (1992), Mixing ratios of carbon monoxide in the troposphere, *J. Geophys. Res.*, *97*(D18), 20,731–20,750.

O'Sullivan, D. (2007), Temporal and Spatial Variability of Halogenated Compounds and Other Trace Gases, Univ. of East Anglia, Norwich, U. K.

Oram, D. E., F. S. Mani, J. C. Laube, M. J. Newland, C. E. Reeves, W. T. Sturges, S. A. Penkett, C. A. M. Brenninkmeijer, T. Röckmann, and P. J. Fraser (2011), Long-term tropospheric trend of octafluorocyclobutane (c-C4F8 or PFC-318), *Atmos. Chem. Phys. Discuss.*, *11*(7), 19,089–19,111, doi:10.5194/acpd-11-19089-2011.

Park, M., W. J. Randel, L. K. Emmons, P. F. Bernath, K. A. Walker, and C. D. Boone (2008), Chemical isolation in the Asian monsoon anticyclone observed in Atmospheric Chemistry Experiment (ACE-FTS) data, *Atmos. Chem. Phys.*, *8*(3), 757–764, doi:10.5194/acp-8-757-2008.

Park, M., W. J. Randel, L. K. Emmons, and N. J. Livesey (2009), Transport pathways of carbon monoxide in the Asian summer monsoon diagnosed from Model of Ozone and Related Tracers (MOZART), *J. Geophys. Res.*, *114*, D08303, doi:10.1029/2008JD010621.

Qian, W., and D.-K. Lee (2000), Seasonal march of Asian summer monsoon, *Int. J. Climatol.*, *20*(11), 1371–1386, doi:10.1002/1097-0088(200009)20:11<1371::AID-JOC538>3.0.CO;2-V.

Rudolph, J. (1995), The Tropospheric Distribution and Budget of Ethane, *J. Geophys. Res.*, *100*(D6), 11,369–11,381, doi:10.1029/95JD00693.

Russo, R. S., et al. (2003), Chemical composition of Asian continental outflow over the western Pacific: Results from Transport and Chemical Evolution over the Pacific (TRACE-P), *J. Geophys. Res.*,*108*(D20), 8804, doi:10.1029/2002JD003184.

Scheele, M. P., P. C. Siegmund, and P. F. J. Van Velthoven (1996), Sensitivity of trajectories to data resolution and its dependence on the starting point: In or outside a tropopause fold, *Meteorol. Appl.*, *3*(3), 267–273, doi:10.1002/met.5060030308.

Schuck, T. J., C. A. M. Brenninkmeijer, F. Slemr, I. Xueref-Remy, and A. Zahn (2009), Greenhouse gas analysis of air samples collected onboard the CARIBIC passenger aircraft, *Atmos. Meas. Tech.*, *2*(2), 449–464, doi:10.5194/amt-2-449-2009.

Singh, H. B., D. Ohara, D. Herlth, W. Sachse, D. R. Blake, J. D. Bradshaw, M. Kanakidou, and P. J. Crutzen (1994), Acetone in the atmosphere: Dis-

tribution, sources, and sinks, *J. Geophys. Res.*, *99*(D1), 1805–1819, doi:10.1029/93JD00764.

Singh, H. B., M. Kanakidou, P. J. Crutzen, and D. J. Jacob (1995), High concentrations and photochemical fate of oxygenated hydrocarbons in the global troposphere, *Nature*, *378*(6552), 50–54, doi:10.1038/378050a0.

Singh, H. B., et al. (1996), Reactive nitrogen and ozone over the western Pacific: Distribution, partitioning, and sources, *J. Geophys. Res.*, *101*(D1), 1793–1808, doi:10.1029/95JD01029.

Slemr, F., R. Ebinghaus, P. G. Simmonds, and S. G. Jennings (2006), European emissions of mercury derived from long-term observations at Mace Head, on the western Irish coast, *Atmos. Environ.*, *40*(36), 6966–6974, doi:10.1016/j.atmosenv.2006.06.013.

Slemr, F., et al. (2009), Gaseous mercury distribution in the upper troposphere and lower stratosphere observed onboard the CARIBIC passenger aircraft, *Atmos. Chem. Phys.*, *9*(6), 1957–1969, doi:10.5194/acp-9-1957-2009.

Streets, D. G., K. F. Yarber, J. H. Woo, and G. R. Carmichael (2003), Biomass burning in Asia: Annual and seasonal estimates and atmospheric emissions, *Global Biogeochem. Cycles*, *17*(4), 1099, doi:10.1029/2003GB002040.

Tang, J. H., L. Y. Chan, C. C. Chang, S. Liu, and Y. S. Li (2009), Characteristics and sources of non-methane hydrocarbons in background atmospheres of eastern, southwestern, and southern China, *J. Geophys. Res.*, *114*, D03304, doi:10.1029/2008JD010333.

Wang, S. F., X. B. Feng, G. G. Qiu, L. H. Shang, P. Li, and Z. Q. Wei (2007), Mercury concentrations and air/soil fluxes in Wuchuan mercury mining district, Guizhou province, China, *Atmos. Environ.*, *41*(28), 5984–5993, doi:10.1016/j.atmosenv.2007.03.013.

Weigelt, A., M. Hermann, P. F. J. van Velthoven, C. A. M. Brenninkmeijer, G. Schlaf, A. Zahn, and A. Wiedensohler (2009), Influence of clouds on aerosol particle number concentrations in the upper troposphere, *J. Geophys. Res.*, *114*, D01204, doi:10.1029/2008JD009805.

Woo, J. H., et al. (2003), Contribution of biomass and biofuel emissions to trace gas distributions in Asia during the TRACE-P experiment, *J. Geophys. Res.*, *108*(D21), 8812, doi:10.1029/2002JD003200.

Wu, Y., D. G. Streets, S. X. Wang, and J. M. Hao (2010), Uncertainties in estimating mercury emissions from coal-fired power plants in China, *Atmos. Chem. Phys.*, *10*(6), 2937–2946, doi:10.5194/acp-10-2937-2010.

A. K. Baker, C. A. M. Brenninkmeijer, T. J. Schuck, and F. Slemr, Max Planck Institute for Chemistry, Air Chemistry Division, J.-J.-Becherweg 27, D-55128 Mainz, Germany. (angela.baker@mpic.de)

S. C. Lai, South China University of Technology, School of Environmental Science and Engineering, Guangzhou University City, Guangzhou 510006, China.

D. E. Oram, National Centre for Atmospheric Science, School of Environmental Sciences, University of East Anglia, Norwich, NR4 7TJ, UK.

P. van Velthoven, Royal Netherlands Meteorological Institute (KNMI), P.O. Box 201, De Bilt NL-3730 AE, Netherlands.

A. Zahn, Institut für Meteorologie und Klimaforschung (IMK), Forschungszentrum Karlsruhe, Weberstr. 5, D-76133 Karlsruhe, Germany.

H. Ziereis, Institut für Physik der Atmosphäre, Deutsches Zentrum für Luft- und Raumfahrt, Oberpfaffenhofen, D-82234 Wessling, Germany.